Available online at www.sciencedirect.com
SCIENCE DIRECT
ELSEVIER
Polymer 46 (2005) 1685–1692
polymer
www.elsevier.com/locate/polymer

Formation mechanism of shish in the oriented melt (II)—two different growth mechanisms along and perpendicular to the flow direction

Shinichi Yamazaki[a,*], Kaori Watanabe[b], Kiyoka Okada[b], Koji Yamada[c], Katsuharu Tagashira[c], Akihiko Toda[b], Masamichi Hikosaka[b]

[a]*Faculty of Environmental Science and Technology, Okayama University 3-1-1 Tsushima-Naka, Okayama 700-8530, Japan*
[b]*Faculty of Integrated Arts and Sciences, Hiroshima University, 1-7-1 Kagamiyama, Higashi Hiroshima 739-8521, Japan*
[c]*R&D Department, Kawasaki Development Center, SunAllomer Ltd, 3-2 Yako 2-chome, Kawasaki-ku, Kawasaki 210-8548, Japan*

Received 21 May 2004; received in revised form 7 December 2004; accepted 7 December 2004
Available online 8 January 2005

Abstract

In part 1 of this series of paper, we have solved the formation mechanism of shish from the oriented melt based on the kinetic observation. In this work, we have shown for the first time the molecular mechanism of the growth of shish by kinetic study. We found that there are two different type of the growth of shish against the flow direction. The growth rate along the flow direction (U) is proportional to ΔT, where ΔT is the degree of supercooling. This indicates that U is mainly controlled by the rearrangement process of the chain near the end surface of the shish. On the other hand, the growth rate perpendicular to the flow direction (V) obeyed a well-known equation $V \propto \exp(-B/\Delta T)$, where B is a constant proportional to the free energy necessary for forming a critical secondary nucleus ΔG^*. This indicates that V is mainly controlled by the secondary nucleation process on the side surface of shish. Moreover, we also found that there is a critical shear rate $\dot{\gamma}^*$ for the growth of shish. Below $\dot{\gamma}^*$, U and V approached to zero and the growth rate of spherulite, respectively. From this experimental fact, we proposed that the chain conformation near the interface between the melt and shish, i.e. near the end and side surface of shish is elongated and oriented by the shear flow above $\dot{\gamma}^*$.

Keywords: Growth; Shish; Shear flow

1. Introduction

We have solved the formation mechanism of shish based on the kinetic study in previous paper (part 1) [1]. In this paper, we will solve the growth mechanism of shish under continuous shear flow based on the kinetic study for the first time.

1.1. Formation mechanism of shish

In our previous study [1], we have shown the first direct evidence that the shish was formed from the bundle nucleus within the oriented melt as shown in Fig. 1(A). The bundle nucleus was formed from elongated chains within the oriented melt caused by pins. Then, the bundle nucleus grows to the shish from the root of pins along the flow direction. This indicates that the formation of shish is controlled by the nucleation process. Moreover, we also found that there exists a critical shear rate of the formation of shish. Based on these experimental facts, we have solved the molecular mechanism of formation of shish. When we focus to shish formed by fixed pins, there is advantage that we can identify the position of shish and measure the size of focused shish. Because shish formed at a floating dusts will run away from eye field immediately.

1.2. Growth mechanism of shish

Purpose of this work is to solve the molecular mechanism of the growth of shish based on the kinetic observations. Based on this mechanism, we will show the chain

* Corresponding author. Tel.: +81 86 251 8901; fax: +81 86 251 8901.
E-mail address: zaki@cc.okayama-u.ac.jp (S. Yamazaki).

0032-3861/$ - see front matter © 2004 Elsevier Ltd. All rights reserved.
doi:10.1016/j.polymer.2004.12.010

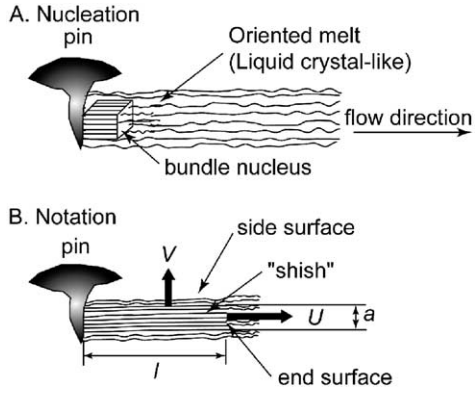

Fig. 1. Schematic illustration of (A) nucleation of bundle nucleus within the oriented melt, (B) notation of growth rate U and V.

conformation within the interface between the shish and the melt. Fig. 1(B) shows the notation for the growth of shish. We can define two different growth rates of shish in regard to the chain axis in the shish, i.e. along the flow direction (U) and perpendicular to the flow direction (V). It is reasonable to consider that U and V are controlled by different mechanisms of growth. The U may be controlled by the rearrangement of the chains on the end surface of shish. Because it is difficult to nucleate on the end surface of shish due to a lot of loop or cilia chains. For this growth direction, a few schematic models have been proposed [2,3]. However, as far as author's knowledge, the molecular mechanism based on kinetic study has not been done yet. On the other hand, the V may be controlled by the secondary nucleation and growth on side surface of shish. For kebab growth on shish, it has been accepted that the growth mechanism is the same as that of spherulite under quiescent state. However, the growth mechanism of shish has not been solved yet. We emphasis that no reports have been shown what is the rate determining process such as nucleation or rearrangement for the growth mechanism of shish.

1.3. ΔT dependence of growth rate R

If the growth rate R is controlled by the rearrangement or nucleation process, R is given as follows.

For rearrangement [4–6]

$$R \propto \Delta T \tag{1}$$

For nucleation [7,8]

$$R \propto \exp(-\Delta G^*/kT) \propto \exp(-B/\Delta T) \tag{2}$$

where ΔT is the degree of supercooling defined by

$$\Delta T = T_m^0 - T_c \tag{3}$$

where T_m^0 is the equilibrium melting temperature and T_c is the crystallization temperature and k is the Boltzmann constant and T is temperature and B is a constant. B is proportional to the free energy of necessary for forming a critical secondary nucleus ΔG^*. In Eq. (2), B is given by [9]

$$B = \frac{4b_0\sigma\sigma_e T_m^0}{3kT\Delta h} \tag{4}$$

where σ is the side surface free energy and σ_e is the end surface free energy and b_0 is a height of nucleus and Δh is the heat of fusion. From Eq. (4), we can obtain σ within the oriented melt (σ^{ori}).

1.4. Competition between chain elongation and conformational relaxation

Under the shear flow, it is considered that the effects of chain elongation caused by pins and conformational relaxation are always competing. As mentioned in Section 1.1, we have shown that there exists a critical shear rate $\dot{\gamma}^*$ for the formation of shish [1]. In other words, this indicates that there exists a $\dot{\gamma}^*$ for the primary nucleation with bundle nucleus. As well as in the case of the formation of shish, it is expected that there exists a $\dot{\gamma}^*$ for the growth of shish. If the shear rate $\dot{\gamma}$ will decrease, the behavior of growth of shish will significantly change. When the chain relaxation is dominant rather than the chain elongation in the case of low $\dot{\gamma}$, it is expected that U and V will approach to zero and growth rate of spherulite V_{sp} under quiescent state, respectively. Therefore, we can define $\dot{\gamma}^*$ for the growth of shish. From the growth behavior of shish near $\dot{\gamma}^*$, we will propose the chain conformation within the interface between the melt and shish.

1.5. Purpose of this work

First purpose of this study is to solve the growth mechanism of shish based on the ΔT dependence of U and V. Second purpose is to show the model for the chain conformation near the end and side surface of shish from the experimental fact that there exists $\dot{\gamma}^*$ for the growth of shish.

2. Experimental

2.1. Samples

The samples used in this work were linear iPP (PM600A supplied by SunAllomer Ltd: $M_w = 25.0 \times 10^4$, $M_w/M_n = 3.57$) and PE (JPE0 supplied by SunAllomer Ltd: $M_w = 11.6 \times 10^4$, $M_w/M_n = 2.42$), where M_w and M_n are weight and number average molecular weights, respectively.

2.2. Instruments

Crystallization under shear flow and quiescent state was observed by using a hotstage (Linkam, CSS-450). The geometry of the hotstage is parallel plate (bottom plate is rotating). The range of $\dot{\gamma}$ and the gap between both plates h were 0–5 s^{-1} and 100 μm, respectively. Observation of

growth behavior was carried out by means of a polarizing optical microscope.

2.3. Measurements

In order to obtain the ΔT dependence of U and V of shish, we measured the length of shish along the flow direction l and thickness of shish a. The shish is effectively generated one dimensionally by artificial pins described in our previous paper [1]. Therefore, we can measure the length of shish l between the root of pin and the growth front. For measurement of a, we measured a at the same position of focused shish. This can be actually achieved when one end of shish is fixed by pins. Our original experimental idea that shish is formed by fixed pins has advantage for measurement of l and a. We can define U and V as $U \equiv \mathrm{d}l/\mathrm{d}t$ and $V \equiv \mathrm{d}a/2\mathrm{d}t$, respectively, where t is the time. The T_m^0 of PE under shear flow and quiescent state were almost the same as shown in our previous paper [10]. We assume that T_m^0 of iPP under shear flow and quiescent state are also the same [1]. The ranges of ΔT were 40.2–49.2 K for iPP and 9.1–15.1 K for PE, respectively.

3. Results

3.1. Shish was formed on the root of pins and grew to the flow direction

In order to confirm that the shish is formed on the root of pins and grow to the flow direction, we carried out a simple examination. If the shish will be formed on the root of pins and grow to the flow direction, growth direction of shish should depend on the flow direction. In other words, when the flow direction will be reversed, we can find that growth direction of shish should be reversed. As shown in Fig. 2, it was found that the growth direction of shish was reversed when the flow direction was changed to opposite direction. Therefore, it is confirmed that the shish is formed on the root of pins and grew to the flow direction.

3.2. ΔT dependence of l vs. t

Fig. 3 shows that l of iPP and PE linearly increased with increase of t. It is noted here that $t=0$ is defined that the time when a shish is formed is equal to zero. This t dependence of l indicates that the U can be regarded as the stationary growth. Therefore, we can obtain U from the slope of this straight line. For both iPP and PE, U increased with increase of ΔT.

3.3. ΔT dependence of a vs. t

Fig. 4 shows that a of iPP and PE linearly increased with increase of t. This t dependence of a indicates that the V can be also regarded as the stationary growth. Therefore, we can obtain V from the slope of this straight line. For both iPP and PE, V increased with increase of ΔT as well as U.

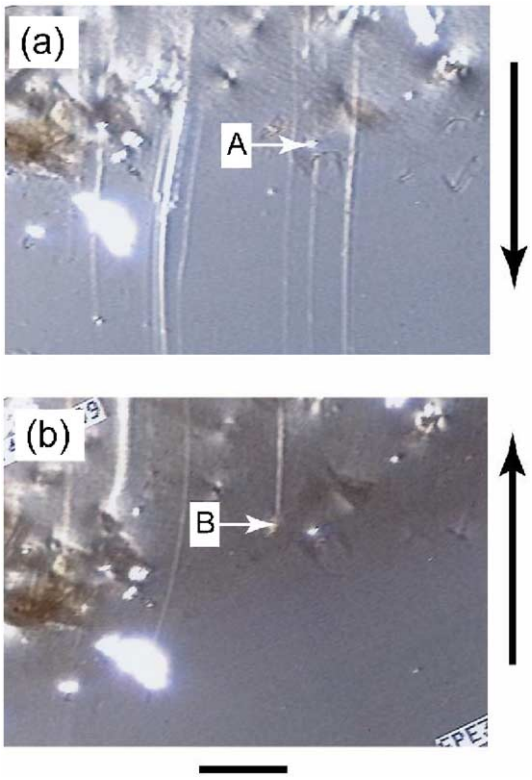

Fig. 2. Typical polarizing optical micrograph. Growth direction is coincident with the flow direction indicated by arrows. A and B indicate the root of pins.

3.4. T_c dependence of U and V

Fig. 5 shows the plots of U and V against T_c. It was found that U and V significantly increased with decrease of T_c and approached to zero near T_m^0. Since the T_c dependence of V is stronger than that of U, it is expected that the functional form of U and V as a function of ΔT is significantly different. Since V rapidly increased with decrease of T_c comparing with U, V may exponentially increase with increase of ΔT. On the other hand, U may fit with the much weak ΔT dependent function such as ΔT.

3.5. ΔT dependence of U

We have shown in Fig. 5(A) and (B) that U is proportional to ΔT. As mentioned in Section 1.2, it is difficult to nucleate on the end surface of shish. According to the classical nucleation theory [9], the necessary condition of the surface nucleation is; (1) flat surface with atomic scale and (2) existence of facet. For the end surface of shish, both conditions are not satisfied. Therefore, it is considered that the mechanism of U should be rearrangement process of the chains near the end surface of shish. For both iPP and PE, it was found that U is fitted by

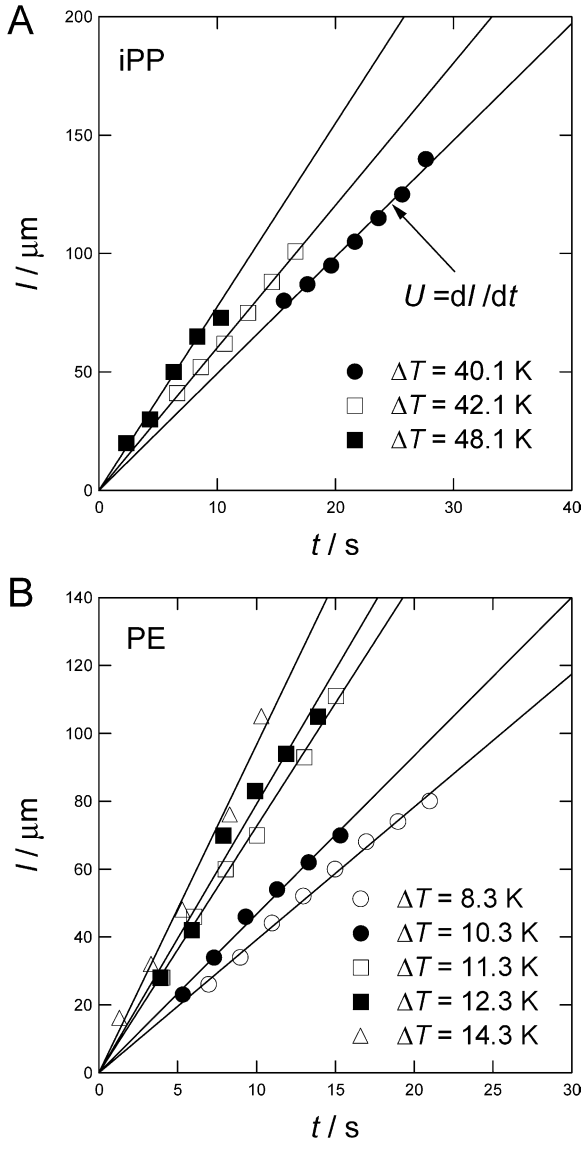

Fig. 3. Plots of l of (A) iPP and (B) PE against t. U is defined by the slope of the straight line.

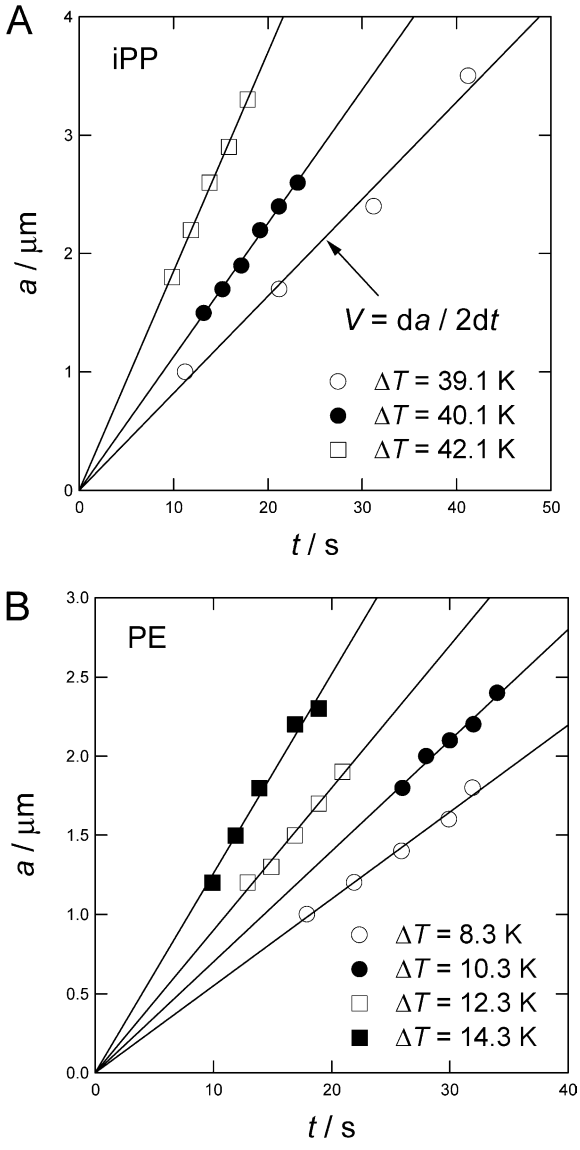

Fig. 4. Plots of a of (A) iPP and (B) PE against t. V is defined by the half of slope of the straight line.

$$U \propto \Delta T \tag{5}$$

Therefore, we concluded that U is mainly controlled by the rearrangement process of the chains [4–6].

3.6. ΔT dependence of V

Figs. 6(A) and 7(A) show the plot of V against $1/\Delta T$. For both iPP and PE, it was found that V is fitted by

$$V \propto \exp(-B/\Delta T) \tag{6}$$

Therefore, we concluded that V is mainly controlled by the secondary nucleation process [7,8].

3.7. $\dot{\gamma}$ dependence of U and V

Fig. 8 shows the plots of U and V of iPP against $\dot{\gamma}$ at $\Delta T = 41.8$ K. It was found that U and V increase from zero and V_{sp} under quiescent state [11] with increase of $\dot{\gamma}$, respectively. Both U and V increased with increase of $\dot{\gamma}$, and then saturated for $\dot{\gamma} > 1\ s^{-1}$. We defined $\dot{\gamma}^*$ for the growth of shish where $U(\dot{\gamma}^*)$ and $V(\dot{\gamma}^*)$ are equal to half value of saturated value of U and V. We obtained $\dot{\gamma}^*$ as

$$\dot{\gamma}^* = 0.3\ s^{-1} \tag{7}$$

3.8. l stops increasing below $\dot{\gamma}^*$ and restarts increasing with step up of $\dot{\gamma}$

Fig. 9 shows the plot of l against t when $\dot{\gamma}(>\dot{\gamma}^*)$ was decreased to below $\dot{\gamma}^*$ and then increased above $\dot{\gamma}^*$ at a constant $\Delta T = 41.8$ K. It was found that in the case of $\dot{\gamma} > \dot{\gamma}^*$, l linearly increased with increase of t. Once $\dot{\gamma}$ jumped to below $\dot{\gamma}^*$, l stopped increasing. Then, $\dot{\gamma}$ jumped

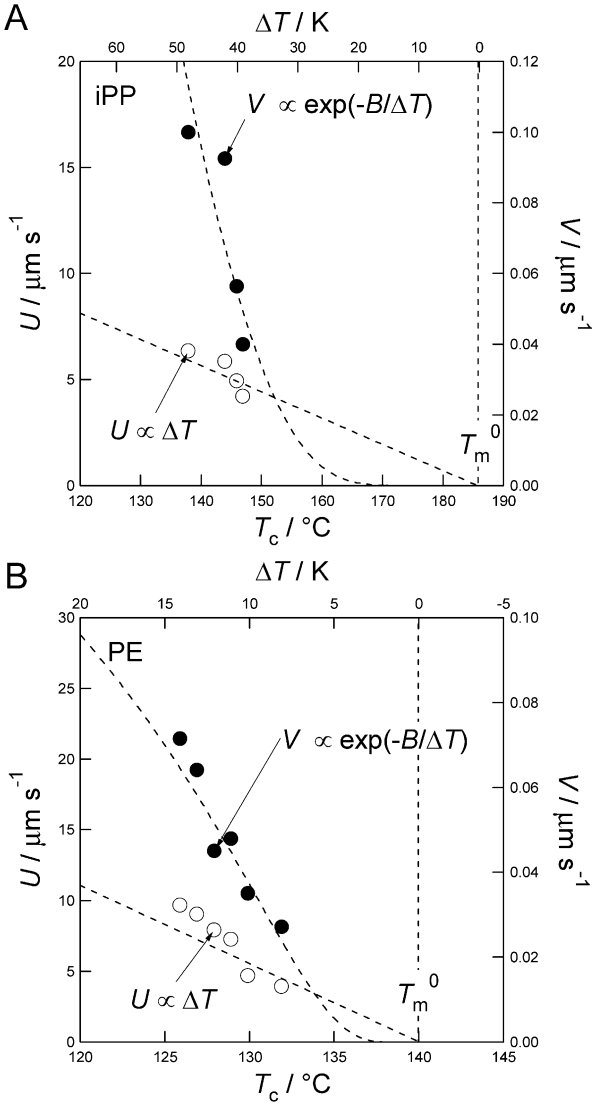

Fig. 5. Plots of U and V of (A) iPP and (B) PE against T_c.

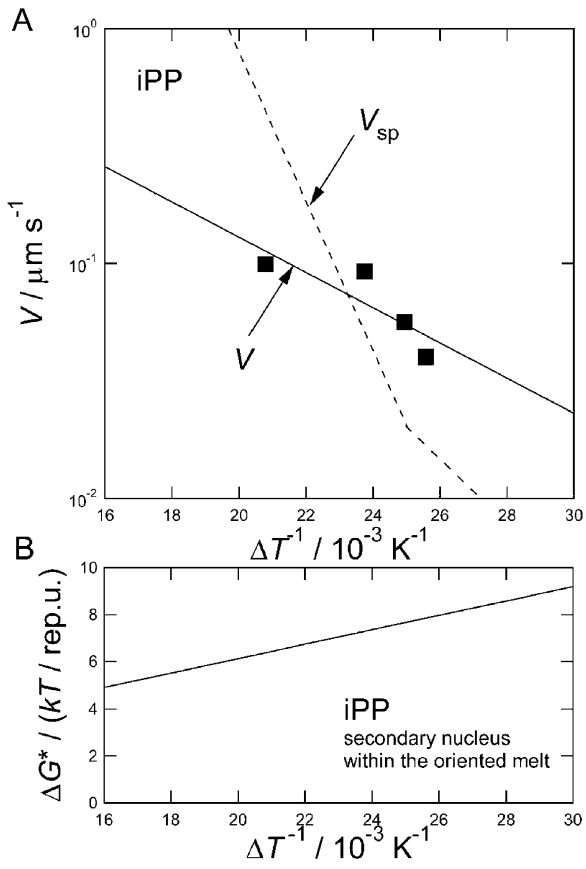

Fig. 6. (A) Plots of V of iPP against ΔT^{-1}. (B) Plot of ΔG^* of iPP against ΔT^{-1}.

to above $\dot{\gamma}^*$, l started increasing again. This confirmed that there exists $\dot{\gamma}^*$ for the growth U of shish.

4. Discussion

4.1. Growth mechanism along U

Fig. 10 shows a schematic illustration of the chain conformation near the end surface of shish at $\dot{\gamma} < \dot{\gamma}^*$ ($U=0$) and $\dot{\gamma} > \dot{\gamma}^*$ ($U>0$). In the case of $\dot{\gamma} < \dot{\gamma}^*$, on the end surface of shish, there are a lot of loop or cilia chains. These chains can be regarded as relaxed random coils. On the other hand, in the case of $\dot{\gamma} > \dot{\gamma}^*$, on the end surface of shish, a lot of loop or cilia chains are elongated by the shear flow and the oriented melt is formed. The origin of this elongation is that the entangled chains are moved by the shear flow. In the former case, since it is difficult to rearrange the chain conformation near the end surface of shish, the growth U can not progress. On the other hand, in the latter case, since it is easy to rearrange the chain conformation due to the elongation, the growth U can progress and the new growth front will be made.

4.2. Growth mechanism along V

Fig. 11 shows a schematic illustration of the chain conformation near the side surface of shish at $\dot{\gamma} < \dot{\gamma}^*$ and $\dot{\gamma} > \dot{\gamma}^*$. In general, it can be assumed that the side surface of shish is smooth and flat. Therefore, a lot of free random coils will repeat to adsorb and detach on the side surface of shish. In the case of $\dot{\gamma} < \dot{\gamma}^*$, the chains adsorbed on the side surface do not orient so much. The growth V will progress by the surface nucleation. In this case, it is considered that the growth mechanism along V is essentially the same as the lateral growth of spherulite under quiescent state. In other words, the side surface free energy σ^{ori} around the secondary nucleus does not change and is almost the same as that within the isotropic melt under quiescent state (σ^{iso}). On the other hand, in the case of $\dot{\gamma} > \dot{\gamma}^*$, the chains adsorbed on the side surface will be elongated by the shear flow. Since the chains are oriented along the flow direction,

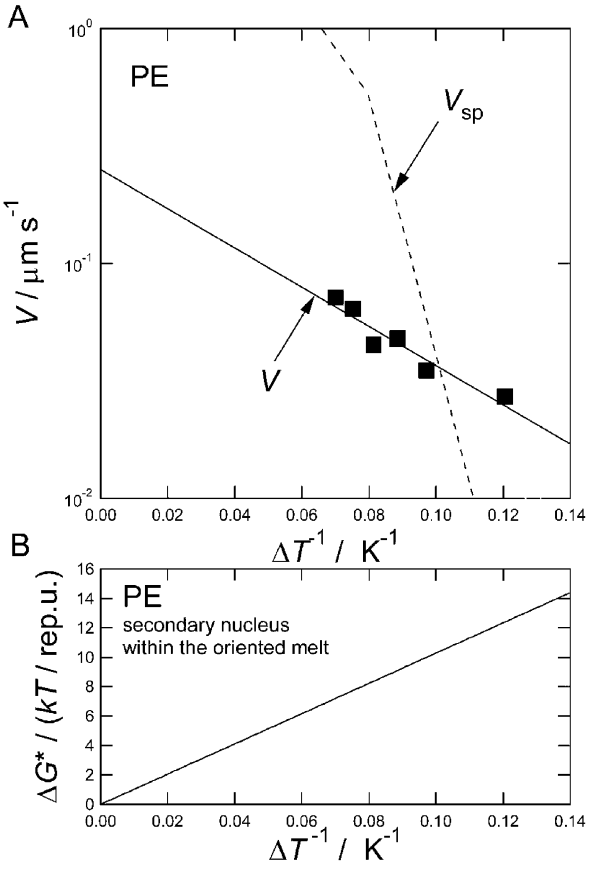

Fig. 7. (A) Plots of V of PE against ΔT^{-1}. (B) Plot of ΔG^* of PE against ΔT^{-1}.

σ^{ori} will decrease. In this case, V increases comparing with that at $\dot{\gamma} < \dot{\gamma}^*$ due to small σ^{ori}.

4.3. Side surface free energy within the oriented melt

As shown in part 1 of this series of paper [1], the bundle

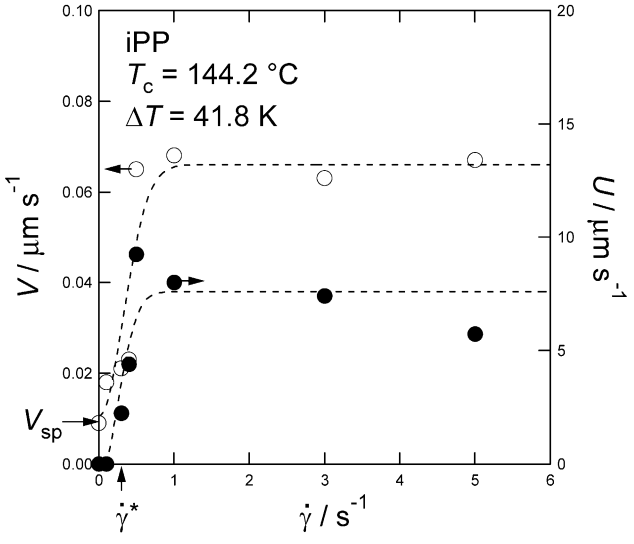

Fig. 8. Plots of U and V of iPP against $\dot{\gamma}$ at ΔT=41.8 K.

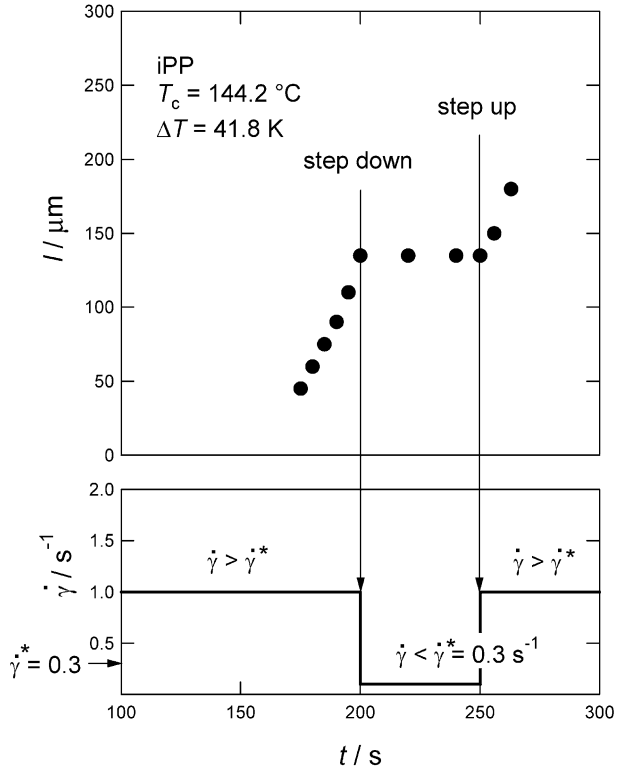

Fig. 9. The effect of step up and down of $\dot{\gamma}$ on l of iPP at ΔT=41.8 K.

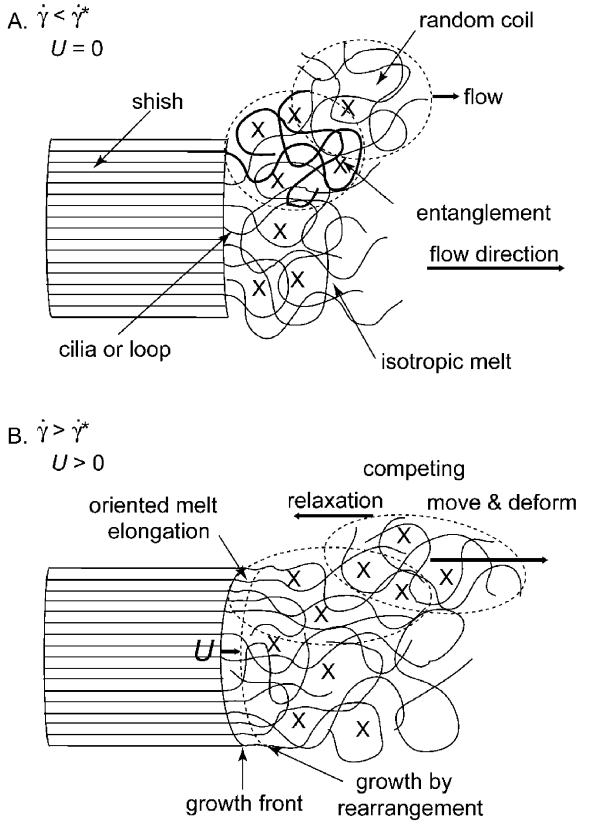

Fig. 10. Schematic illustration of the chain conformation near the end surface of shish at (A) $\dot{\gamma} < \dot{\gamma}^{**}$ (U=0) and (B) $\dot{\gamma} > \dot{\gamma}^*$ (U>0).

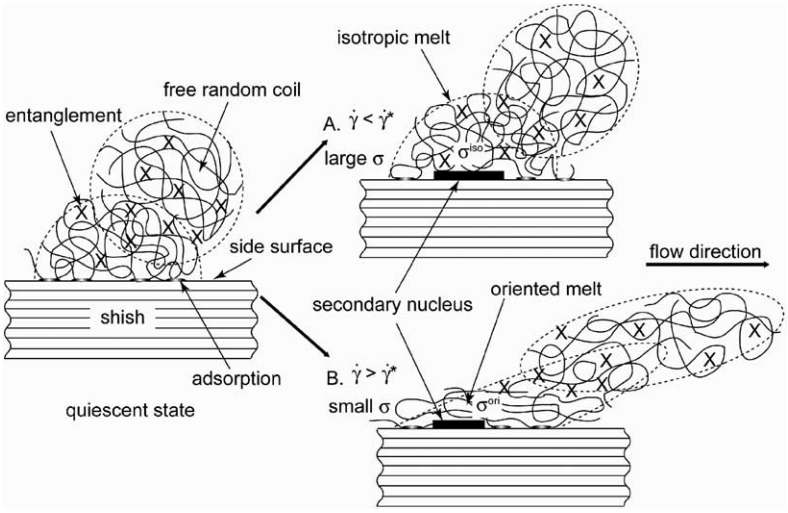

Fig. 11. Schematic illustration of the chain conformation near the side surface of shish at (A) $\dot{\gamma} < \dot{\gamma}^*$ and (B) $\dot{\gamma} > \dot{\gamma}^*$.

nucleus will be formed on the root of pins since the chains are strongly elongated near the pins. Let us consider which type of nucleus such as bundle or fold nucleus will be formed on the side surface of shish. As shown in Fig. 11, the chains near the side surface of shish repeat to adsorb and detach on the side surface of shish under the shear flow. The chains will be weakly elongated and not be fully extended. It can be regarded as the partially oriented melt. Therefore, it is reasonable to consider that the fold nucleus will be formed from the partially oriented melt. Because it is difficult to form the bundle nucleus within the partially oriented melt due to weak chain elongation.

Assuming that the crystal form in the case of secondary nucleus on the side surface of shish is the same as that in the case of spherulite under quiescent and the end surface free energy of fold nucleus σ_e^f is applicable to the case of the nucleation from the partially oriented melt, we can derive simple relation from Eq. (4) as,

$$\frac{B_{sh}}{B_{sp}} = \frac{\sigma^{ori}}{\sigma^{iso}} \tag{8}$$

where B_{sh} and B_{sp} are the slope of the straight line of the plots of V and V_{sp} against ΔT^{-1} and σ^{ori} and σ^{iso} are the side surface free energy within the oriented and isotropic melt, respectively. From Eq. (8), using σ^{iso} reported in literature [12,13] and experimental B_{sp} [11,14] shown in Figs. 6(A) and 7(A), we can calculate σ^{ori} as

$$\begin{aligned} \sigma^{ori} &= 6.5 \times 10^{-3}\ (\mathrm{J/m^2}) \quad \text{for iPP} \\ &= 2.6 \times 10^{-3}\ (\mathrm{J/m^2}) \quad \text{for PE} \end{aligned} \tag{9}$$

Here, the parameters used in this calculation were summarized in Table 2 in part 1 of this series of paper[1]. Comparing with σ^{iso} (12×10^{-3} J/m^2 for iPP and 14×10^{-3} J/m^2 for PE), it was found that σ^{ori} in this work is smaller than σ^{iso}. Because the structural difference between the oriented melt and a nucleus is much smaller than that between the isotropic melt and a nucleus.

4.4. ΔT dependence of ΔG^* of V

Using σ^{ori} in this work and σ_e^f reported in literatures [13, 15–17], we can calculate ΔG^* for the secondary nucleation on the side surface of shish against ΔT^{-1} as shown in Figs. 6(B) and 7(B).

$$\begin{aligned} \Delta G^* &= 307 \times 10^3/\Delta T\ (kT/\text{rep.unit}) \quad \text{for iPP} \\ &= 67 \times 10^2/\Delta T\ (kT/\text{rep.unit}) \quad \text{for PE} \end{aligned} \tag{10}$$

In all range of ΔT, we concluded that the growth of shish perpendicular to the flow direction is mainly controlled by the nucleation process since a criterion that $\Delta G^* \gg 2\,kT$ was satisfied.

5. Conclusion

1. The growth of shish along the flow direction is mainly controlled by the rearrangement process of the chains within the oriented melt.
2. The growth of shish perpendicular to the flow direction is mainly controlled by the secondary nucleation process of fold nucleus within partially oriented melt.
3. There exists a critical shear rate $\dot{\gamma}^*$ for the growth of shish. $\dot{\gamma}^* \approx 0.3\ \mathrm{s^{-1}}$ for iPP.

Acknowledgements

This work was partly supported by Grant-in-Aid for JSPS Fellow (No. 08115) and Scientific Research on Priority Areas B2 (No. 12127205) and Scientific Research A2 (No. 12305062) from the Ministry of Education, Culture, Sports,

Science and Technology, Japan. The synchrotron radiation experiments were performed at the BL40B2 in the SPring-8 (Harima) with approval of the Japan Synchrotron Radiation Research Institute (JASRI) and the BL10C in the Photon Factory (KEK; Tsukuba).

References

[1] Yamazaki S, Watanabe K, Okada K, Yamada K, Tagashira K, Toda A, Hikosaka M. (Part 1), Polymer 2005:46.
[2] Pennings AJ. J Polym Sci, Polym Symp 1977;59:55–86.
[3] Lieberwirth I, Loos J, Petermann J, Keller A. J Polym Sci, Polym Phys 2000;38:1183–7.
[4] Frenkel J. Z Physik Sovietunion 1932;1:498–500.
[5] Cormia RI, Mackenzie JD, Turnbull D. J Appl Phys 1963;34: 2239–44.
[6] Turnbull D. Thermodynamics in physical metallurgy.: American Society for Metals; 1950.
[7] Becker R, Döring W. Ann Phys 1935;24:719–52.
[8] Turnbull D, Fisher JC. J Chem Phys 1949;17:71–3.
[9] Price FP. Nucleation in polymer crystallization. In: Zettlemoyer AC, editor. Nucleation. New York: Marcel Dekker; 1969. Chapter 8.
[10] Yamazaki S, Hikosaka M, Toda A, Wataoka I, Yamada K, Tagashira K. J Macromol Sci 2003;B42:499–512.
[11] Yamada K, Hikosaka M, Toda A, Tagashira K, Submitted to Polymer.
[12] Cheng SZD, Janimak JJ, Zhang A, Cheng HN. Macromolecules 1990; 23:298–303.
[13] Hoffman JD, Frolen LJ, Ross GS, Lauritzen Jr. JI. J Res NBS 1975;671–99.
[14] Okada M, Nishi M, Takahashi M, Matsuda H, Toda A, Hikosaka M. Polymer 1998;39:4535–9.
[15] Yamada K, Hikosaka M, Toda A, Yamazaki S, Tagashira K. Macromolecules 2003;36:4790–801.
[16] Yamada K, Hikosaka M, Toda A, Yamazaki S, Tagashira K. Macromolecules 2003;36:4802–12.
[17] Yamada K, Hikosaka M, Toda A, Yamazaki S, Tagashira K. J Macromol Sci 2003;B42:733–52.